Optics Letters

Enhancement cavities for few-cycle pulses

N. Lilienfein,[1,2,*] C. Hofer,[1,3] S. Holzberger,[1,4] C. Matzer,[5] P. Zimmermann,[5] M. Trubetskov,[1] V. Pervak,[2] and I. Pupeza[1]

[1]Max-Planck-Institut für Quantenoptik, Hans-Kopfermann-Strasse 1, 85748 Garching, Germany
[2]Ludwig-Maximilians-Universität München, Am Coulombwall 1, 85748 Garching, Germany
[3]Technische Universität München, James-Franck-Str. 1, 85748 Garching, Germany
[4]Present address: Menlo Systems GmbH, Am Klopferspitz 19a, 82152 Martinsried, Germany
[5]Layertec GmbH, Ernst-Abbe-Weg 1, 99441 Mellingen, Germany
*Corresponding author: nikolai.lilienfein@mpq.mpg.de

Received 28 October 2016; revised 9 December 2016; accepted 9 December 2016; posted 9 December 2016 (Doc. ID 279669); published 11 January 2017

We address the challenge of increasing the bandwidth of high-finesse femtosecond enhancement cavities and demonstrate a broad spectrum spanning 1800 cm^{-1} (195 nm) at −10 dB around a central wavelength of 1050 nm in an EC with an average finesse exceeding 300. This will benefit a host of spectroscopic applications, including transient absorption spectroscopy, direct frequency comb spectroscopy, and Raman spectroscopy. The pulse circulating in the EC is composed of only 5.4 optical cycles, at a kilowatt-level average power. Together with a suitable gating technique, this paves the way to the efficient generation of multi-megahertz-repetition-rate isolated extreme ultraviolet attosecond pulses via intracavity high-order harmonic generation.

OCIS codes: (140.4780) Optical resonators; (320.0320) Ultrafast optics; (310.1620) Interference coatings; (140.7240) UV, EUV, and X-ray lasers; (300.6340) Spectroscopy, infrared.

https://doi.org/10.1364/OL.42.000271

Owing to their unique properties, passive optical resonators, or enhancement cavities (ECs), have leveraged a number of breakthrough achievements in spectroscopy. First, the path length enhancement for the interaction with a weakly absorbing sample provided by ECs has enabled sensing techniques with unparalleled sensitivity [1,2]. Second, in state-of-the-art ECs, broadband optical frequency combs or, equivalently, the ultrashort pulses produced by frequency-stabilized mode-locked lasers, can be enhanced in power by a few orders of magnitude. In addition to boosting the sensitivity of broadband (transient) absorption spectroscopy [3–7], this affords intensities high enough to drive nonlinear processes such as high-harmonic generation (HHG) at multi-megahertz repetition rates [8–14]. Recently, this has enabled the extension of direct frequency comb spectroscopy to the vacuum ultraviolet [10,11] and the demonstration of the feasibility of extreme ultraviolet frequency combs with photon energies exceeding 100 eV [12,14]. Finally, by detuning the input frequency comb with respect to the longitudinal modes of a high-finesse EC, individual comb lines can be resolved via spectral filtering, leading to the highest frequency resolution achievable in broadband spectroscopy so far [15–17].

The sensitivity enhancement underlying the success of ECs in spectroscopy applies not only to absorption, but also to the spectral phase [18]. In combination with the spectral phase the curvature inherent to standard dielectric multilayer mirrors, this sensitivity limits the optical bandwidth of ECs. The broadest bandwidths of ECs reported hitherto in literature amount to 60 nm at a central wavelength of 800 nm [8], and to 100 nm at a central wavelength of 1050 nm [19], both demonstrated in ECs with a finesse of about 300. Significantly extending the spectral coverage and shortening the pulse duration in femtosecond ECs would tremendously benefit existing applications and enable novel ones. For instance, cavity-enhanced Raman spectroscopy, which so far has only been demonstrated in narrowband ECs [20,21] could provide high-sensitivity trace gas detection, covering a significant part of the molecular fingerprint region in a single measurement. Another example is cavity-enhanced HHG. Here, the attainable photon energy and flux have been shown to scale with the decreasing duration of the driving pulse [12,14,19,22]. Together with a suitable gating technique, intracavity pulses approaching the few-cycle regime could enable the efficient generation of bright isolated attosecond pulses at megahertz repetition rates [23,24]. This would dramatically reduce the acquisition time in pump-probe experiments involving the detection of charged particles [25].

In this Letter, we report on an EC with an average finesse exceeding 300, which supports a 10 dB bandwidth of 195 nm (1800 cm^{-1}) centered at 1050 nm. We measure intracavity pulse duration of 19 fs (5.4 cycles) and an average power of 1.04 kW, limited by the seeding laser system. To accomplish this bandwidth increase by a factor of 2 over state-of-the-art femtosecond ECs, we address challenges related to the mirror design, production, and characterization, as well as to the cavity setup and intracavity pulse characterization.

The design and the production of multilayer cavity mirrors that significantly surpass the bandwidth of standard

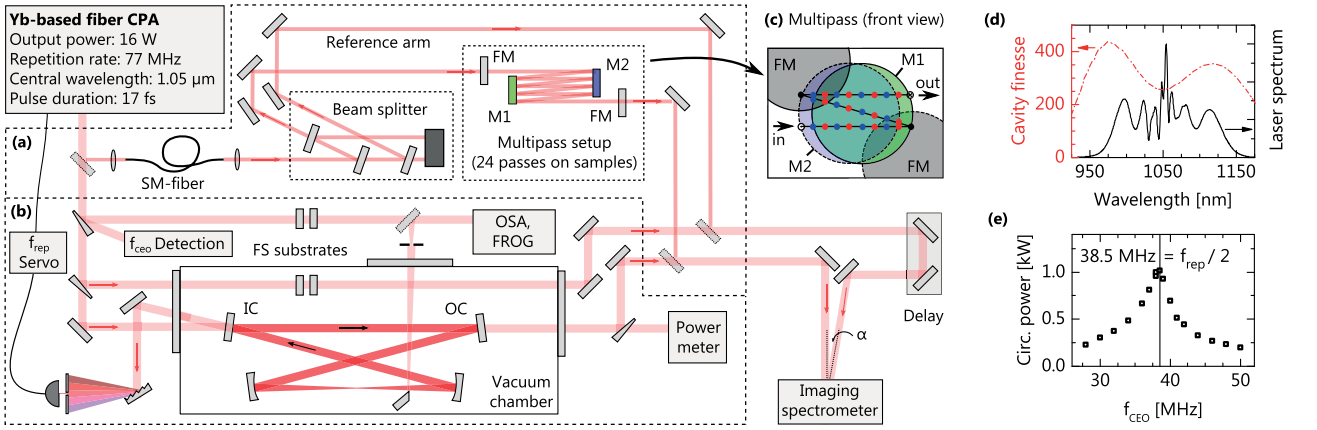

Fig. 1. (a) Setup for multipass SSI measurements. (b) Setup for enhancement cavity (EC) experiments. The cavity includes two partially reflective mirrors (IC, OC). (c) Front view of the multipass setup illustrating the beam path. Two unprotected gold-coated folding mirrors are used to achieve 24 reflections (blue and red dots) on two sample mirrors (M1, M2). (d) Output spectrum of the laser and the finesse of the EC. (e) Intracavity power for the different values of the laser f_{CEO}.

quarter-wave stacks are challenging. Designs of such coatings typically exhibit a very low tolerance with respect to thickness variations in production. This results in deviations of the phase characteristics of the produced coatings from the design and variations among individual coating deposition runs of the same design. Efficient enhancement is only possible if the spectral phase accumulated during one round-trip in the cavity deviates by less than approximately π/F from a linear phase (F = Finesse). Thus, for a four-mirror cavity with $F = 300$, the maximum acceptable phase deviation per mirror is about 2.5 mrad, which is far less than typical errors for broadband coatings. However, an EC with a suitable round-trip phase can be built by combining mirrors from several coating runs. This approach renders a reliable pre-characterization of the mirror phase with a precision of a few milliradians indispensable. To this end, we measure the accumulated spectral phase from multiple reflections on two 1"-diameter sample mirrors using spatial-spectral interferometry (SSI) [26].

Figure 1 shows the overall experimental setup. The Yb-based chirped-pulse fiber amplification system, previously described in [27], delivers 180 fs pulses at 77 MHz. The spectrum is broadened in a photonic-crystal fiber (NKT, LMA-25) and compressed to 17 fs in a double-angle chirped-mirror setup, with an output average power of 16 W. For the mirror-characterization setup [Fig. 1(a)], a small fraction of this power is coupled to a single-mode fiber for spatial filtering. The transmitted light is then collimated and split into a sample and a reference arm in a setup composed of three partially reflective mirrors produced in the same coating deposition run, placed under a small angle of incidence (AOI). This beam splitting setup ensures that the beams in both arms accumulate the same phase from substrates and from the coatings of the transport mirrors. The sample beam is subjected to a total of 24 reflections on two 1" sample mirrors [Fig. 1(c)]. The AOI on the sample mirrors is 1.5°. Thus, the polarization dependence is negligible. The reference and the sample beams intersect at the entrance slit of an imaging spectrometer, producing interferograms from which the accumulated spectral phase difference can be retrieved [26]. Figure 2(a) shows the spectral phase of a reference measurement of two unprotected gold mirrors. The maximum deviation from the expected flat phase is less than 1.5 mrad.

Novel cavity mirrors with a reflectivity $R > 99.995\%$ (highly reflective, HR) and $R = 99 \pm 0.3\%$ (partially reflective, PR) in the wavelength range between 950 and 1150 nm were designed and produced (Layertec GmbH). The design goal was group delay dispersion (GDD) in reflection of 0 fs^2 with deviations within ± 1 fs^2 over this bandwidth. Nb_2O_5 and SiO_2 were chosen as coating materials. The theoretical round-trip spectral

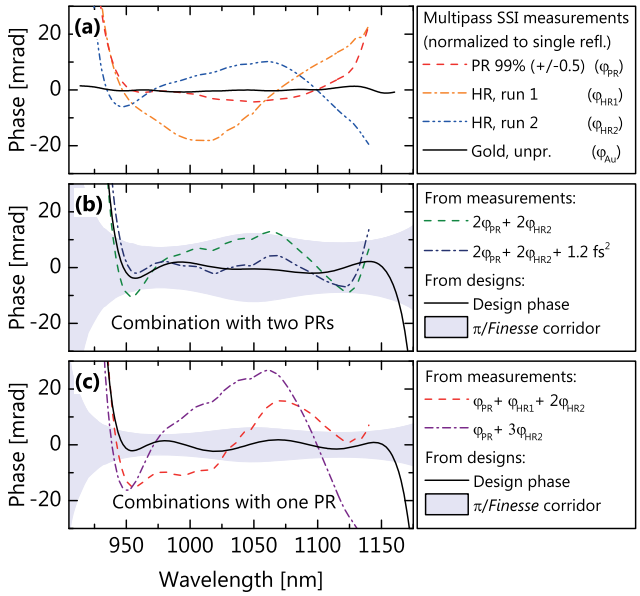

Fig. 2. (a) Spectral phase retrieved from multipass SSI measurements of three different multilayer mirror coatings (PR, partially reflective; HR, highly reflective) and a bare gold coating. (b) Sum of the measured spectral phases (green; blue: with an additional positive GDD of 1.2 fs^2) and of the corresponding coating designs (black) of a mirror combination suitable for a four-mirror impedance-matched EC. (c) Sum of the measured spectral phases (red, purple) and of the corresponding coating designs (black), of the mirror combinations suitable for an input-coupler limited four-mirror EC.

phase of a four-mirror cavity with these mirror designs is shown in Figs. 2(b) and 2(c), for an impedance-matched configuration and an input-coupler limited configuration, respectively. The production process was optimized to achieve an absolute thickness deviation of below 0.5 nm per layer and a maximum spatial inhomogeneity of 0.1% over a diameter of 10 mm on each substrate. Two coating runs (HR1, HR2) were performed with the HR design. For the PR mirror coating, the positioning of the substrates in the machine was chosen to achieve a graded distribution of spectral shifts of the GDD curve.

Figure 2(a) shows phase measurements of the three produced coatings. The measured spectral phases deviate significantly from the designs. The spectral phases of the PR and the HR2 coatings have similar curvatures with opposite signs. In Fig. 2(b), the sum of the measured spectral phases for two of each of these coatings is shown. The resulting curve represents the single-round-trip phase in a four-mirror impedance-matched cavity. It lies mostly within the π/F-corridor calculated from the measured transmission of the PR coatings. The remaining negative curvature of the phase corresponds to a GDD of about -1.2 fs^2. Figure 2(c) illustrates that an input-coupler limited EC with only one PR is not viable with these mirror coatings: the combination of a higher finesse and a worse shape of the spectral phase does not allow for a broadband enhancement.

Figure 1(b) depicts the setup used for the cavity-based experiments. The impedance-matched cavity is composed of two HR2-coated mirrors with a radius of curvature of 600 mm and two flat PR mirrors used as input- and output-coupling mirrors (IC, OC, respectively). The finesse of the impedance-matched cavity, as calculated from transmission measurements of the PR coating, and the laser spectrum are shown in Fig. 1(d). The reflections off two thin fused silica (FS) wedges are used for the detection of the carrier-envelope offset frequency f_{CEO}, for pulse characterization and for the reference arm of cavity-SSI measurements. In the SSI reference arm, two uncoated FS substrates compensate for the dispersion of the IC and OC substrates in the sample arm. The repetition frequency of the laser is locked to the EC using the Pound–Drever–Hall scheme. For the generation of the error signal, a narrow part of the laser spectrum at a wavelength of about 1000 nm is chosen. A D-shaped silver mirror is used to clip a small part of the intracavity light (<0.1%) to circumvent the spectral filtering and phase of the cavity mirrors in transmission for pulse characterization. The clipped beam is spatially filtered using a pinhole. Since the cavity mode size is not wavelength independent, the measured spectra have to be corrected for the clipping efficiency. The beam transmitted through the OC is used for the SSI sample arm and to measure a portion P_{leak} as a diagnostic for the intracavity power. The intracavity power is calculated accounting for the spectrally varying transmission of the PR coating $T_{\mathrm{PR}}(\lambda)$ and the intracavity spectrum $I(\lambda)$:

$$P_{\mathrm{circ}} = P_{\mathrm{leak}} \frac{\int I(\lambda)\mathrm{d}\lambda}{\int I(\lambda) T_{\mathrm{PR}}(\lambda)\mathrm{d}\lambda}. \quad (1)$$

In a first experiment, the optimal offset frequency [19] of the cavity in vacuum is determined. Figure 1(e) shows P_{circ} for a scan of the laser f_{CEO}. It peaks at 38.5 MHz, corresponding to $f_{\mathrm{rep}}/2$. The intracavity spectrum for this f_{CEO} is plotted in Fig. 3(a). The 10 dB spectral bandwidth is 168 nm. The intracavity average power was 950 W, and the average power

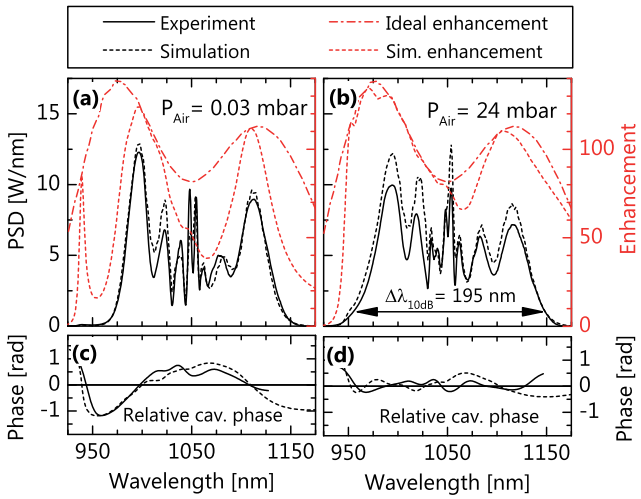

Fig. 3. Measured and calculated intracavity spectra, and calculated spectral enhancement in vacuum (a) and with 24 mbar of air pressure (b). The spectral enhancement is shown for an "ideal" dispersion-free cavity and for the mirror phase shown in Fig. 2. (c,) (d) Measured and calculated cavity phase.

enhancement factor was 68. The spectral phase of the intracavity pulses with respect to the incoming light [Fig. 3(c)] is measured via SSI. The negative curvature of the cavity round-trip phase can be compensated for by adding some dispersive material to the cavity. In our setup, this can be conveniently achieved by flooding the vacuum chamber with a small amount of ambient air. At an air pressure of about 24 mbar in the chamber, we obtain the broadest spectral bandwidth in the EC. To exploit this increased bandwidth, we slightly broaden the input spectrum. Figure 3(b) shows the resulting intracavity spectrum exhibiting a 10 dB bandwidth of 195 nm. Here, the average power was 1040 W with an average power enhancement of 75.

Figure 3 also shows the spectral enhancement and phase calculated with the phase data from the multipass measurements (Fig. 2), without additional dispersion [Figs. 3(a) and 3(c)], and with an additional GDD of 1.2 fs^2 [Figs. 3(b) and 3(d)]. From these and the experimental input laser spectra, intracavity spectra are calculated. The good agreement of both simulated cavity spectra and phase curves with the experiment confirms the accuracy and utility of the multipass SSI measurements.

The laser pulse compression is optimized to achieve minimal pulse duration in the cavity. We characterize the intracavity pulse using two independent methods. First, we retrieve the pulse from second-harmonic-generation frequency-resolved optical gating (FROG) measurements of the clipped intracavity beam. The resulting spectral phase has to be corrected for the spectral phase of the vacuum chamber window. Additionally, we retrieve the intracavity pulses' spectral phase from FROG measurements of the input pulse, together with SSI measurements of the relative cavity phase. Here, two fused silica substrates in front of the FROG device account for the dispersion of the vacuum chamber window and the input coupler (Fig. 1). To calculate the pulse duration, the intracavity spectrum is measured independently. The results of the retrieval in the frequency and in the time domain are shown in Figs. 4(b) and 4(c). The full-width at half-maximum intensity pulse durations determined from the first and second methods are 18.8 and 19 fs, respectively, for the EC in vacuum

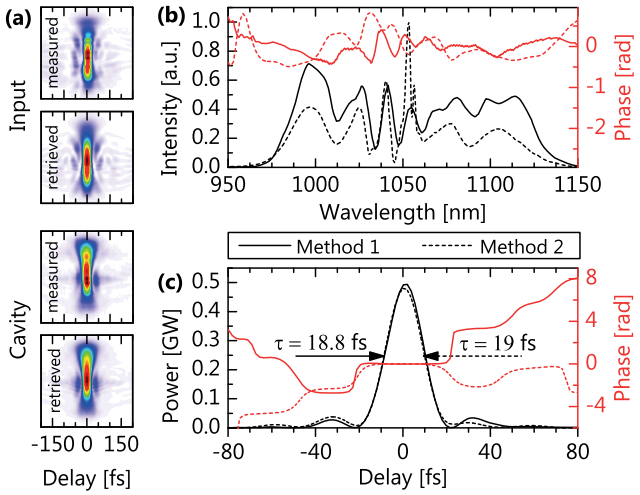

Fig. 4. (a) Measured and retrieved FROG traces of input and cavity pulses. The FROG errors were 0.008 and 0.005, respectively. (b) Intracavity spectra and spectral phases calculated by both methods. (c) Corresponding temporal intensities and phases.

(Fourier limit: 17.5 fs). The peak power of the intracavity pulse is about 0.5 GW.

In conclusion, we have demonstrated methods enabling high-finesse ECs that substantially surpass the state-of-the-art in bandwidth and support pulses approaching the few-cycle range. While a robust coating design and an accurate deposition is of utmost importance, the current error margins in production can only be overcome by combining mirrors from several coating runs. To allow for a quick identification of suitable mirror combinations, we have demonstrated a simple multipass setup capable of measuring the spectral phase of mirrors with, to the best of our knowledge, an unprecedented precision of 1.5 mrad. Further, we have presented methods for the reliable characterization of pulses in such cavities and measured pulses of sub-20 fs duration. We increased the bandwidth of this EC to about 1800 cm^{-1} by fine-tuning the cavity dispersion with the air pressure in the vacuum chamber. For applications that do not allow the presence of a gas, the same effect can be reached by a thin plate placed under Brewster's angle in the EC, e.g., a 56 μm fused silica or a 7 μm Si_3N_4 plate.

The intracavity bandwidth reported here will immediately benefit a host of broadband spectroscopy schemes. For instance, femtosecond stimulated Raman spectroscopy [28] with this cavity would cover half the molecular fingerprint region without the need for tuning. Furthermore, the demonstrated pulse duration, together with a suitable gating technique [24], promises to enable the efficient generation of isolated attosecond pulses via HHG for time-resolved experiments in attosecond physics at multi-megahertz repetition rates.

Funding. Deutsche Forschungsgemeinschaft (DFG) (MAP); Fraunhofer-/Max-Planck-Gesellschaft Cooperation (MEGAS); European Research Council (ERC) (617173).

Acknowledgment. The authors thank the fiber laser group at the Institute of Applied Physics at Friedrich-Schiller-University Jena for providing the laser. They also thank T. Saule and M. Högner for helpful discussions.

REFERENCES

1. J. Hodgkinson and R. P. Tatam, Meas. Sci. Technol. **24**, 012004 (2013).
2. G. Gagliardi and H.-P. Loock, *Cavity-Enhanced Spectroscopy and Sensing* (Springer, 2014).
3. T. Gherman and D. Romanini, Opt. Express **10**, 1033 (2002).
4. B. Bernhardt, A. Ozawa, P. Jacquet, M. Jacquey, Y. Kobayashi, T. Udem, R. Holzwarth, G. Guelachvili, T. W. Hänsch, and N. Picqué, Nat. Photonics **4**, 55 (2009).
5. F. Adler, M. J. Thorpe, K. C. Cossel, and J. Ye, Annu. Rev. Anal. Chem. **3**, 175 (2010).
6. A. Foltynowicz, P. Masłowski, A. J. Fleisher, B. J. Bjork, and J. Ye, Appl. Phys. B **110**, 163 (2013).
7. M. A. R. Reber, Y. Chen, and T. K. Allison, Optica **3**, 311 (2016).
8. C. Gohle, T. Udem, M. Herrmann, J. Rauschenberger, R. Holzwarth, H. A. Schuessler, F. Krausz, and T. W. Hänsch, Nature **436**, 234 (2005).
9. R. Jones, K. Moll, M. Thorpe, and J. Ye, Phys. Rev. Lett. **94**, 193201 (2005).
10. A. Cingöz, D. C. Yost, T. K. Allison, A. Ruehl, M. E. Fermann, I. Hartl, and J. Ye, Nature **482**, 68 (2012).
11. A. Ozawa and Y. Kobayashi, Phys. Rev. A **87**, 022507 (2013).
12. I. Pupeza, S. Holzberger, T. Eidam, H. Carstens, D. Esser, J. Weitenberg, P. Rußbüldt, J. Rauschenberger, J. Limpert, T. Udem, A. Tünnermann, T. W. Hänsch, A. Apolonski, F. Krausz, and E. Fill, Nat. Photonics **7**, 608 (2013).
13. C. Benko, T. K. Allison, A. Cingöz, L. Hua, F. Labaye, D. C. Yost, and J. Ye, Nat. Photonics **8**, 530 (2014).
14. H. Carstens, M. Högner, T. Saule, S. Holzberger, N. Lilienfein, A. Guggenmos, C. Jocher, T. Eidam, D. Esser, V. Tosa, V. Pervak, J. Limpert, A. Tünnermann, U. Kleineberg, F. Krausz, and I. Pupeza, Optica **3**, 366 (2016).
15. C. Gohle, B. Stein, A. Schliesser, T. Udem, and T. W. Hänsch, Phys. Rev. Lett. **99**, 263902 (2007).
16. L. Rutkowski and J. Morville, Opt. Lett. **39**, 6664 (2014).
17. A. Khodabakhsh, V. Ramaiah-Badarla, L. Rutkowski, A. C. Johansson, K. F. Lee, J. Jiang, C. Mohr, M. E. Fermann, and A. Foltynowicz, Opt. Lett. **41**, 2541 (2016).
18. R. J. Jones and J. Ye, Opt. Lett. **27**, 1848 (2002).
19. S. Holzberger, N. Lilienfein, M. Trubetskov, H. Carstens, F. Lucking, V. Pervak, F. Krausz, and I. Pupeza, Opt. Lett. **40**, 2165 (2015).
20. D. J. Taylor, M. Glugla, and R.-D. Penzhorn, Rev. Sci. Instrum. **72**, 1970 (2001).
21. S.-I. Zaitsu, H. Izaki, and T. Imasaka, Phys. Rev. Lett. **100**, 073901 (2008).
22. S. Holzberger, N. Lilienfein, H. Carstens, T. Saule, M. Högner, F. Lücking, M. Trubetskov, V. Pervak, T. Eidam, J. Limpert, A. Tünnermann, E. Fill, F. Krausz, and I. Pupeza, Phys. Rev. Lett. **115**, 023902 (2015).
23. M. Louisy, C. L. Arnold, M. Miranda, E. W. Larsen, S. N. Bengtsson, D. Kroon, M. Kotur, D. Guénot, L. Rading, P. Rudawski, F. Brizuela, F. Campi, B. Kim, A. Jarnac, A. Houard, J. Mauritsson, P. Johnsson, A. L'Huillier, and C. M. Heyl, Optica **2**, 563 (2015).
24. M. Högner, V. Tosa, and I. Pupeza are preparing a manuscript to be titled "Generation of isolated attosecond pulses with enhancement cavities—a theoretical study."
25. M. I. Stockman, M. F. Kling, U. Kleineberg, and F. Krausz, Nat. Photonics **1**, 539 (2007).
26. A. P. Kovács, R. Szipöcs, K. Osvay, and Z. Bor, Opt. Lett. **20**, 788 (1995).
27. T. Eidam, F. Röser, O. Schmidt, J. Limpert, and A. Tünnermann, Appl. Phys. B **92**, 9 (2008).
28. D. R. Dietze and R. A. Mathies, ChemPhysChem **17**, 1224 (2016).